nature nanotechnology

LETTERS

PUBLISHED ONLINE: 19 JANUARY 2014 | DOI: 10.1038/NNANO.2013.285

# A surface-bound molecule that undergoes optically biased Brownian rotation

James A. Hutchison[1,2], Hiroshi Uji-i[1]*, Ania Deres[1], Tom Vosch[3], Susana Rocha[1], Sibylle Müller[4], Andreas A. Bastian[5], Jörg Enderlein[6], Hassan Nourouzi[4], Chen Li[4], Andreas Herrmann[5], Klaus Müllen[4], Frans De Schryver[1] and Johan Hofkens[1,3]*

**Developing molecular systems with functions analogous to those of macroscopic machine components, such as rotors[1,2], gyroscopes[3] and valves[4], is a long-standing goal of nanotechnology. However, macroscopic analogies go only so far in predicting function in nanoscale environments, where friction dominates over inertia[5,6]. In some instances, ratchet mechanisms have been used to bias the ever-present random, thermally driven (Brownian) motion and drive molecular diffusion in desired directions[7]. Here, we visualize the motions of surface-bound molecular rotors using defocused fluorescence imaging, and observe the transition from hindered to free Brownian rotation by tuning medium viscosity. We show that the otherwise random rotations can be biased by the polarization of the excitation light field, even though the associated optical torque is insufficient to overcome thermal fluctuations. The biased rotation is attributed instead to a fluctuating-friction mechanism[8,9] in which photoexcitation of the rotor strongly inhibits its diffusion rate.**

Supramolecular chemistry mediated by non-covalent interactions holds great promise for the rapid and spontaneous assembly of molecular devices at an interface[10–12]. With this goal in mind we designed molecular device components **1**–**3** (Fig. 1a). They each consist of a tetraphenylmethane unit which is functionalized with three quaternized aniline moieties and a chromophoric rylene derivative at the 4-positions of the phenyl rings. In **1**, a perylene monoimide chromophore is directly attached to the tetrahedral core via an ethynylene unit, but in **2** and **3** an additional phenylene spacer is inserted, introducing a tilt angle for the attachment of perylene monoimide and terrylene monoimide chromophores, respectively (see Supplementary Sections 1 and 2 for synthetic methods).

The positively charged trialkylammonium groups and the hydrophobic nature of the extended π-system of the rylene subunits make **1**–**3** amphiphilic structures with potential for directional self-assembly at a negatively charged surface. Figure 1b presents the idealized orientation of energy-minimized representations of **1**–**3**, in which the trialkylammonium groups maximize interaction with a negatively charged surface (here borosilicate glass), forming a tripodal base. In this orientation, **2** and **3** are structural analogues of a macroscopic rotor as the phenylene–ethynylene 'axle' can rotate freely at room temperature[13].

The fluorescent rylene subunits are crucial for detecting the real-time function of **1**–**3**. The visible absorption and emission bands of **2** in ethanol solution are shown in Fig. 1c, associated with a transition dipole in the plane and within a few degrees of the long axis of the rylene subunit, as indicated by the arrows in Fig. 1a. To follow the dynamics of **1**–**3** on glass we used defocused wide-field fluorescence microscopy[14–16], which exploits the distorted image of a molecule's fluorescence at an optical interface to determine the orientation of its transition dipole moment. A library of calculated images for various orientations relative to the interface is shown in Fig. 1d[14].

Defocused wide-field fluorescence microscopy allows many molecules to be analysed simultaneously in the microscope field of view (here 24 μm × 24 μm) with millisecond time resolution. It can resolve both in-plane (azimuthal angle $\varphi$, Fig. 1b) and out-of-plane (polar angle $\theta$, Fig. 1b) transition dipole moment orientations relative to the substrate when quasi-total internal reflection fluorescence (q-TIRF) excitation is used to excite out-of-plane molecular transition dipoles via evanescent fields[16] (see Supplementary Sections 3 and 4 for a full account of experimental and computational methods and the choice of appropriate image integration times for defocused imaging).

Correct orientation upon surface binding is critical for the function of rotors **2** and **3**. A good model to assess surface orientation is provided by **1**, as its perylene imide transition dipole moment is along the long axis of the molecule. Compound **1** is insoluble in nonpolar solvents and aggregates in water, but it dissolves easily in ethanol and methanol. Extremely dilute ($\sim 1 \times 10^{-9}$ M) solutions of **1** in methanol were spin-cast on glass substrates, dispersing the molecules randomly with separations >1 μm. A defocused wide-field fluorescence image of single molecules of **1** on glass is shown in Fig. 2a (q-TIRF excitation used). Characteristic bilobal patterns of emission indicate that the long axis of the molecules lies along the substrate plane (Fig. 2a,c; compare theoretical patterns, $\theta = 90°$, Fig. 1d). The molecules re-orient very rarely and do not translate before photodegradation within 10 s under a nitrogen atmosphere.

However, when an ~100-nm-thick layer of a hydrophobic polymer was spin-cast from toluene on top of molecules of **1** already dispersed on glass (the molecules are not dislodged by nonpolar solvents), the defocused images immediately take on distinctive 'doughnut' shapes, indicating that the long axes of the molecules are preferentially oriented perpendicular to the substrate (Fig. 2b,d; compare theoretical patterns, $\theta = 0$–$30°$ in Fig. 1d). The attraction of the perylene imide subunit to a hydrophobic polymer overlayer (here poly(*n*-butyl methacrylate), PnBMA) is clearly critical for driving the perpendicular orientation of **1** on glass.

[1]Laboratory for Photochemistry and Spectroscopy, Katholieke Universiteit Leuven, Heverlee 3001 Belgium, [2]ISIS & icFRC, Université de Strasbourg & CNRS UMR 7006, Strasbourg 67000, France, [3]Nano-Science Center/Department of Chemistry, University of Copenhagen, Universitetsparken 5, 2100 Copenhagen, Denmark, [4]Synthetic Chemistry Group, Max Plank Institute for Polymer Research, Mainz D-55128 Germany, [5]Department of Polymer Chemistry, Zernike Institute for Advanced Materials, Rijksuniversiteit Groningen, Nijenborgh 4, Groningen 9747 AG, The Netherlands, [6]Drittes Physikalisches Institut, Universität Göttingen, Göttingen D-37077 Germany. *e-mail: Hiroshi.Uji@chem.kuleuven.be; Johan.Hofkens@chem.kuleuven.be

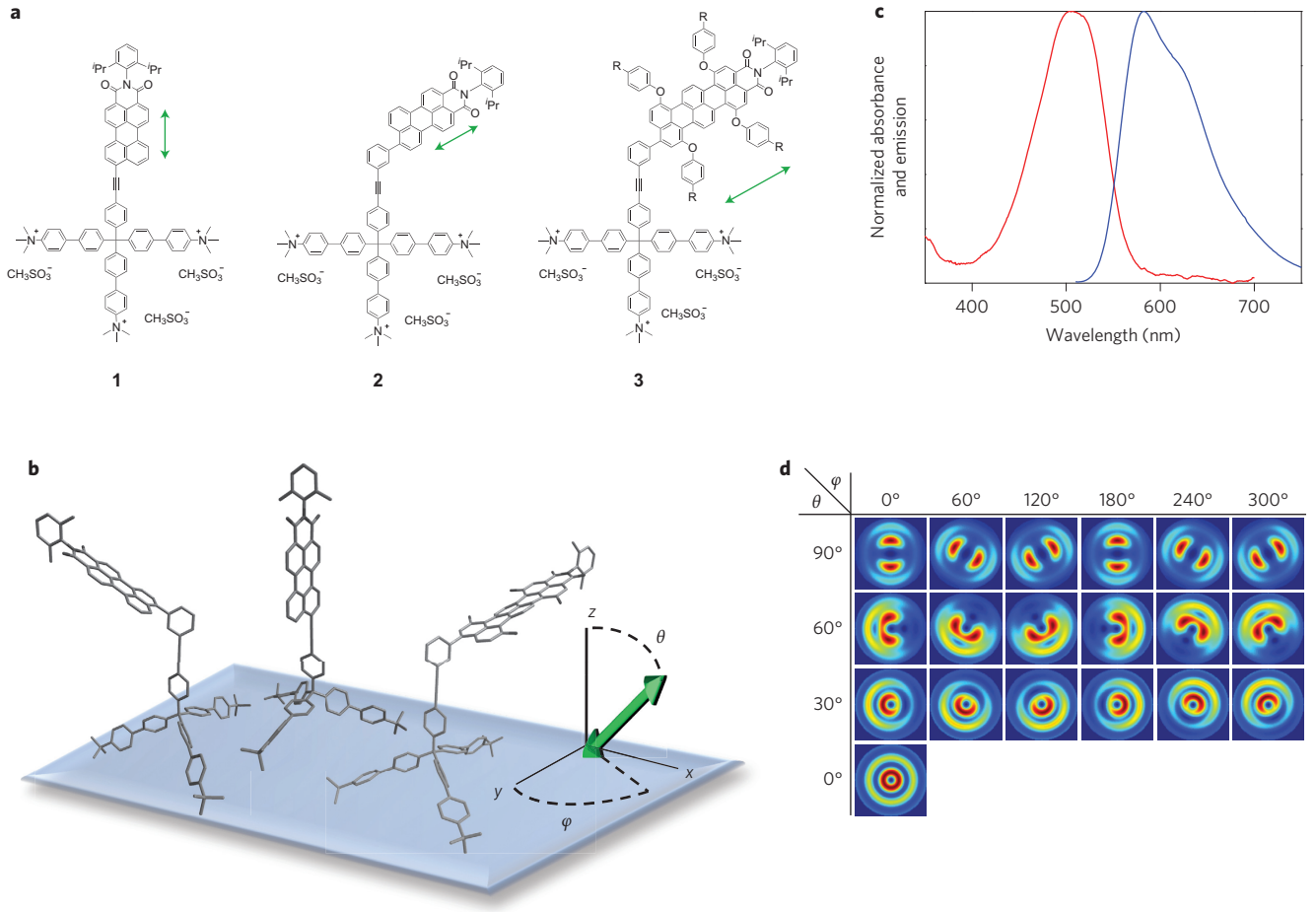


**Figure 1 | Structure and ideal orientation at an interface of molecular device components 1–3. a**, Chemical structures of molecular device components **1–3**. Arrows show the direction of the transition dipole moment in the plane of the rylene monoimide subunits. R = tetramethylbutyl. **b**, Schematic of the ideal orientation of energy-minimized representations of **1–3** at a negatively charged interface (hydrogen atoms and bay position substituents removed for clarity). Cartesian (*x*, *y*, *z*) and polar ($\theta$, $\varphi$) coordinate systems for the orientation of the transition dipole of the rylene subunit relative to the surface are indicated. **c**, Absorption (red) and fluorescence (blue) spectra of **2** in ethanol. **d**, Selection of theoretical defocused emission patterns for a single emitter with transition dipole at various orientations to a glass/air interface (1 μm defocus, 1.3 numerical aperture objective imaging system).

We stress that one cannot distinguish between degenerate representations of the transition dipole unit vector $\mu(\theta, \varphi) = \mu(-\theta, \varphi \pm \pi)$, that is, the two possible perpendicular orientations of **1** in which the perylene subunit is oriented closest to, or furthest away from, the substrate[14]. Nevertheless, given the concerted orientation change observed after applying a hydrophobic polymer overlayer, one must conclude that, in Fig. 2b, the charged 'feet' of the molecules are closest to the substrate and the perylene imide subunit is engulfed by the polymer.

The average orientation of **1** was further optimized by reducing the viscosity of the polymer overlayer by increasing the temperature well above the glass transition temperature ($T_g$) of PnBMA (296 K)[15,16]. At $T = 315$ K, single molecules of **1**, on average, stand up straighter, with a mean polar angle of 19°, compared to 45° at $T = 293$ K (Fig. 2d,e). Polar plots of the orientation of several single molecules of **1** over time show that, although their motions are nearly frozen at $T = 293$ K, at $T = 315$ K most molecules smoothly reorient within a range of low polar angles (0–40°) (Fig. 2f,g).

These results can be understood considering that the free volume available in the polymer is less than the dimensions of **1** (refs 15,16). Below $T_g$, **1** is locked in energetically non-ideal orientations, with jumps in orientation associated with rare polymer matrix motions. Above $T_g$, relaxation of the surrounding polymer chains becomes rapid, and the amphiphiles can reach lower-energy perpendicular orientations. The fact that the average polar angle of **1** is only 19° from the idealized case (Fig. 1b) is an excellent result, given that the phenylene–ethynylene unit itself has limited flexibility[13] and that the heterogeneity of adsorption sites on glass can tilt the molecules. The exceptional ease and speed of fabrication of this process (just two spin-casting steps assemble the molecules over large areas and with arbitrary density on glass) gives this anchoring strategy broad appeal.

Single molecules of **2** were deposited on glass under a PnBMA overlayer as described already. A defocused wide-field fluorescence image of single molecules of **2** under PnBMA at $T = 305$ K is shown in Fig. 3a (q-TIRF excitation used). The majority of molecules have crescent-shaped patterns, indicating that the rylene subunits are oriented with a polar angle of 50–80°, 60° being the ideal case (Fig. 3a; compare with theoretical patterns in Fig. 1d). The low barrier to internal rotation of the phenylene–ethynylene (~2–3 kJ mol$^{-1}$)[13] suggests that, with sufficiently low medium viscosity, the chromophore can rotate independently of the tripodal base at room temperature.

Increasing the temperature to $T_g + 19$ ($T = 315$ K) allowed the rotors to undergo relatively unhindered diffusion (Fig. 3b–d), although only a few molecules survived longer than 20 s and were suitable for accurate correlation analysis[17]. Of these, 40% showed

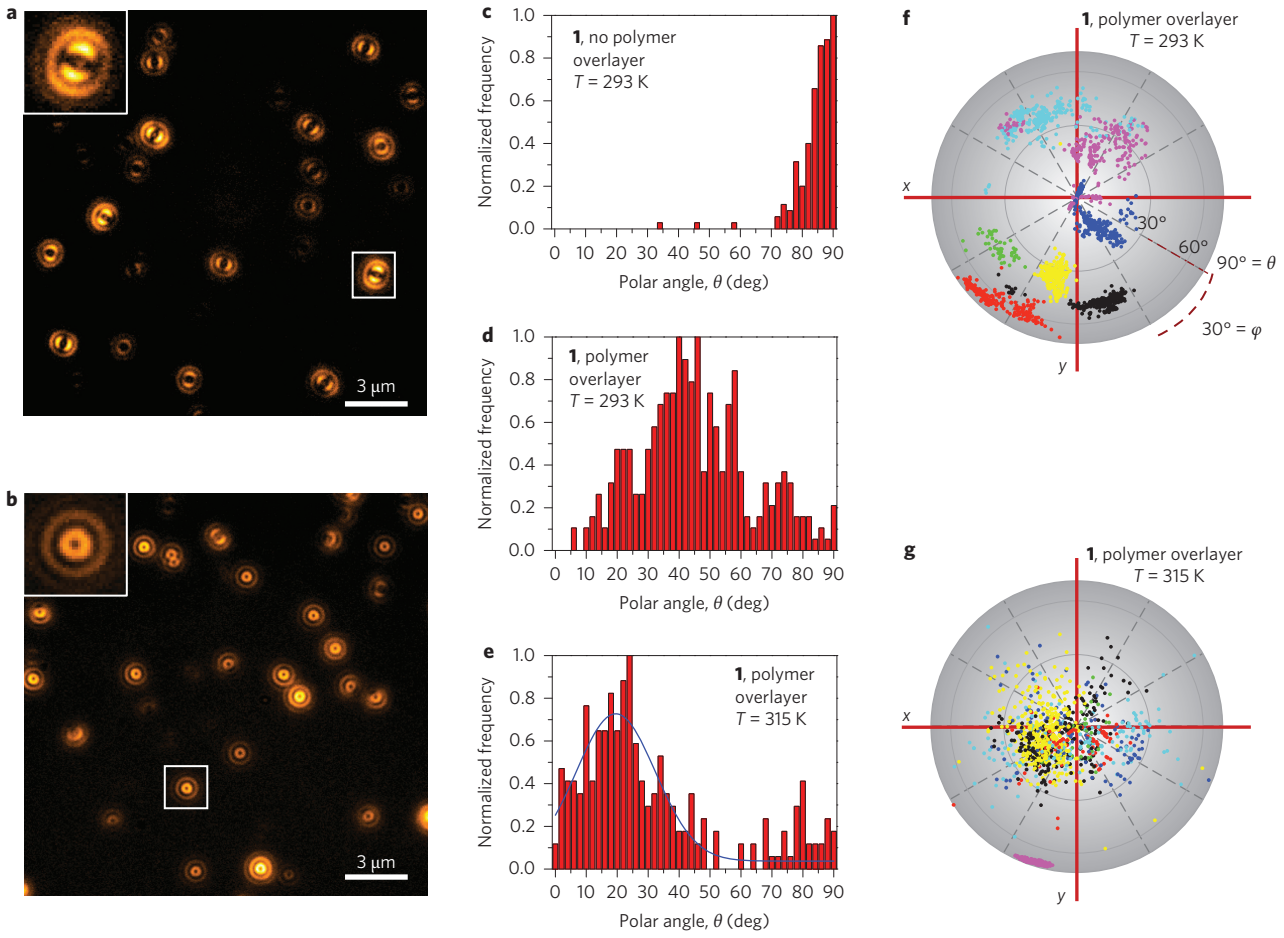


**Figure 2 | Binding of 1 with perpendicular orientation to a glass surface. a**, Defocused wide-field fluorescence images of single molecules of **1** on glass ($T = 305$ K, image integration time 500 ms). Inset: 2.1 × 2.1 μm$^2$ area of the sample with a typical defocused emission pattern. **b**, Images of single molecules of **1** on glass with a ~100-nm-thick overlayer of PnBMA ($T = 305$ K, image integration time 500 ms). Inset: 1.6 × 1.6 μm$^2$ area of the sample with a typical defocused emission pattern. **c**, Normalized frequency histogram of instantaneous polar angle $\theta$ of more than 160 molecules of **1** on glass ($T = 293$ K, image integration time 500 ms, bin width 2°). **d**, Normalized frequency histogram of instantaneous polar angle $\theta$ of more than 160 molecules of **1** on glass under PnBMA ($T = 293$ K, image integration time 500 ms, bin width 2°). **e**, Normalized frequency histogram of instantaneous polar angle $\theta$ of more than 160 molecules of **1** on glass under PnBMA ($T = 315$ K, image integration time 30 ms, bin width 2°). The blue line is a fit of the data to a normal distribution (mean polar angle 19°, full-width at half-maximum of 32°, $R^2 = 0.844$) excluding molecules with $\theta > 70°$, considered to be irreversibly bound parallel to the substrate. **f**, Orientations of seven single molecules of **1** over time on glass under PnBMA ($T = 293$ K; an individual molecule's orientations every 500 ms are represented by dots of a single colour). The polar plot is viewed into the substrate. **g**, Orientation of seven molecules of **1** over time on glass under PnBMA ($T = 315$ K; an individual molecule's orientations every 100 ms are represented by dots of a single colour). An example of a molecule remaining irreversibly bound parallel to the substrate after application of the overlayer is included (magenta points).

the behaviour typified in Fig. 3c. The rylene subunit visits all azimuthal angles with near-equal probability, and the polar angle is predominantly in the range 50–90° (histograms provided in Supplementary Section 5, Supplementary Fig. 2). Examples of single molecules of **2** rotating at $T = 293$ K and $T = 315$ K under PnBMA are provided in Supplementary Movies 1 and 2, respectively.

Autocorrelation functions of the three-dimensional angular displacement ($\Phi$) over time for these molecules were calculated using averages of $\mu(\theta, \varphi, t)\cdot\mu(\theta, \varphi, t + \Delta t)$, the scalar product of the molecules' rylene transition dipole unit vector $\mu$ over a time interval (lag) $\Delta$t (refs 15,17,18). The exponential or near-exponential decay of these rotational autocorrelation functions suggests that these molecules experience a homogeneous environment for rotational diffusion over their survival time (average rotational correlation time, $\tau_c = 0.25$ s; see Fig. 3e and Supplementary Section 5 for analysis). This subset of molecules of **2** thus approximates surface-bound, azimuthal Brownian rotors, displaying random, thermally driven rotational diffusion of their rylene subunit in the substrate plane.

Another subset of molecules of **2** (20%) showed long periods without motion, and the last subset (40%) showed free but heterogeneous diffusion ($\tau_c = 0.99$ s) and a distinctive bias in the azimuthal angle distribution (Fig. 3d, Supplementary Section 5). Intriguingly, the bias in the azimuthal distribution depended on excitation light conditions (investigated in detail in the following).

The fact that a variety of rotation behaviours was observed for **2** is due to the temporal heterogeneity of diffusion environments in the surrounding matrix, which is only sampled for the short survival time of **2** (<20 s). The terrylene monoimide rotor **3** was therefore used, as it is photostable for >20 min under ~2 kW cm$^{-2}$ continuous-wave 640 nm excitation (nitrogen atmosphere). Molecules of **3** were dispersed on glass from ethanol, using a styrene oligomer as an overlayer ($T_g = 277$ K). Experiments were conducted at $T \geq 303$ K to ensure adequate rotational mobility for the rylene subunit. In these conditions, the orientation of the terrylene imide subunit was predominantly in-plane, with polar angles of 60–90°.

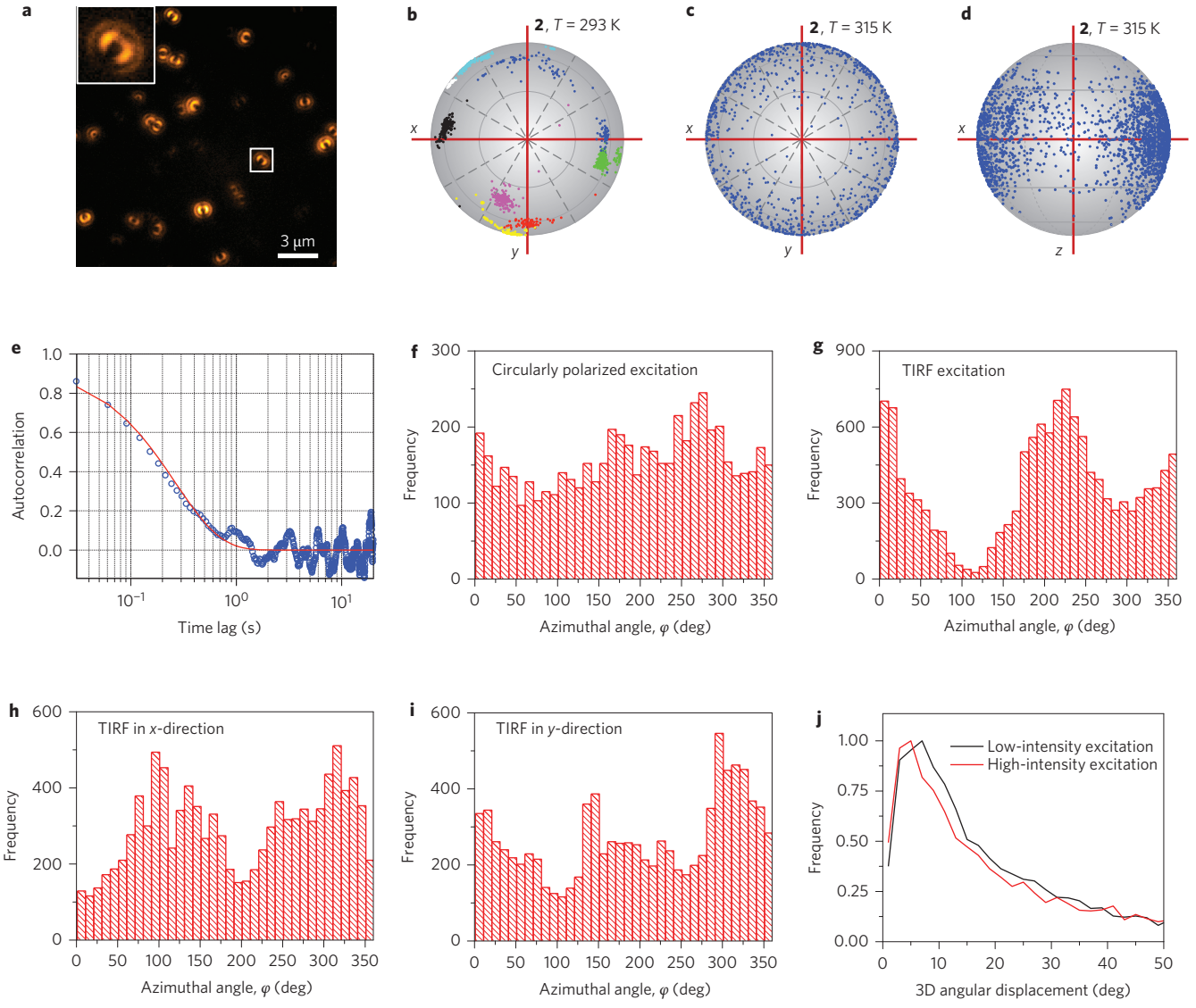


**Figure 3 | Viscosity dependence and optical bias of rotational diffusion of rotors 2 and 3. a**, Defocused wide-field fluorescence image of single molecules of **2** on glass under an ~100 nm PnBMA overlayer ($T = 305$ K, image integration time 500 ms). Inset: 1.7 × 1.7 μm$^2$ region of the sample with a typical defocused emission pattern. **b**, Polar plot of the orientation, over time, of molecules of **2** on glass under PnBMA ($T = 293$ K; an individual molecule's orientations every 500 ms are represented by dots of a single colour). **c**, Polar plot of the orientations, every 30 ms, of a single molecule of **2** on glass under PnBMA ($T = 315$ K). **d**, Polar plot of the orientations, every 30 ms, of a single molecule of **2** on glass under PnBMA ($T = 315$ K). **e**, Autocorrelation function of three-dimensional angular displacement of the single molecule of **2** in **c**. The red line is a fit to a single exponential decay ($\tau_c = 0.26$ s). **f**, Frequency histogram of azimuthal orientations of 25 molecules of **3**, over 15 min, with circularly polarized excitation along the optical axis (styrene oligomer overlayer, $T = 308$ K, image integration time 1 s, bin width 10°). **g**, Frequency histogram of azimuthal orientations of the same 25 molecules of **3** as in **f**, over 15 min, with circularly polarized excitation at high angle to the substrate (q-TIRF). **h**, Frequency histogram of azimuthal orientations of 21 molecules of **3**, over 15 min, with circularly polarized excitation at high angle to the substrate (q-TIRF) such that the evanescent wave propagates in direction *x* along the substrate (10–190° axis in terms of azimuthal angle) (styrene oligomer overlayer, $T = 303$ K, image integration time 0.9 s, bin width 10°). **i**, Frequency histogram of azimuthal orientations of the same 21 molecules of **3** as in **h**, over 15 min, with circularly polarized excitation at high angle to the substrate (q-TIRF) such that the evanescent wave propagates in direction *y* along the substrate (100–280° axis in terms of azimuthal angle). **j**, Frequency histogram of three-dimensional angular displacements for 22 molecules of **3**, over 15 min, at maximum excitation intensity using circularly polarized light aligned on-axis and at 30% of maximum excitation intensity (styrene oligomer overlayer, $T = 308$ K, image integration time 0.8 s, bin width 2°).

Rotation was investigated under two conditions: circularly polarized excitation aligned on-axis (that is, light propagation perpendicular to the substrate) and circularly polarized excitation incident at high angle to the interface (q-TIRF). We compared the frequency histogram of the collected azimuthal angles over time for 25 molecules of **3** with on-axis excitation, and then for the same 25 molecules with q-TIRF excitation (Fig. 3f,g). For on-axis excitation, the azimuthal frequency histogram is flat and the rotors orient in all directions with roughly equal probability. However, for q-TIRF excitation, a similar bias in the azimuthal angle distribution is clearly observed for molecules of **3** as was observed for a subset of molecules of **2**.

Under q-TIRF excitation, the preferential in-plane orientation of the rotors was consistently perpendicular to the direction of propagation of the evanescent field. By changing the direction of light propagation (that is, changing the high-angle approach of the

excitation beam to be along the in-plane *x*- or *y*-direction), alignment of the molecules could be controlled (Fig. 3h,i).

The rotors therefore preferentially align with the strongest in-plane optical field polarization, because the in-plane field distribution for q-TIRF excitation is twice as strong perpendicular to the propagation direction as it is parallel (Supplementary Section 6)[19]. The fact that q-TIRF generates field components in both *y*- and *x*-directions is important, however, as it means one can still track the molecule at all in-plane angles and be sure that the apparent bias is not simply due to non-excitation of the molecule in particular orientations. Supplementary Movie 3 shows single molecules of **3** rotating under the styrene overlayer at $T = 308$ K, with on axis, then q-TIRF, excitation.

It remains to identify the mechanism by which light excitation biases the rotational diffusion of **2** and **3**. Biasing of single dye molecule diffusion with optical gradient forces using resonant excitation has been observed only at power densities 20–100 times higher than the ~2 kW cm$^{-2}$ applied here[20]. Reorientation by optical torque is therefore considered unlikely. Photothermal effects are also unlikely to cause the preferential orientation[21], and rotational diffusion of **3** is faster at lower excitation intensities during on-axis optical excitation (Fig. 3j).

Another possibility is a fluctuating-friction mechanism, in which changes in molecule–matrix interactions or molecular conformation upon photoexcitation lead to molecular diffusion slowing down greatly[8,9]. In this case, diffusion rates become excitation intensity-dependent, and under polarized excitation a freely rotating molecule tends to align its transition dipole with the optical field vector because, at that orientation, it has the highest probability of being excited and its diffusion rate slowing.

Strong evidence for significant electronic redistribution in the excited state of **2** and subsequent matrix reorganization is provided by its broad spectral features and 322 meV Stokes-shifted emission (Fig. 1c), typical of 'push–pull' rylene imides substituted directly at the electron-poor core by electron-rich aryl substituents (without core substitution, rylene imides show structured fluorescence with 30 meV Stokes shift)[22–25]. Such rylene based push–pull systems form charge transfer states on photoexcitation that can be emissive. Transient absorption spectra of **2** in solution are also consistent with photoinduced intramolecular charge transfer state formation (see Supplementary Section 7 for the photophysics of **1**–**3**).

Transfer of electron density from the phenylene–ethynylene to the rylene in the excited state of **2** and **3** could slow rotational diffusion in several ways. It would dramatically restrict axle function, as the barrier to torsion of the phenylene–ethynylene increases from 2.4 to 24 kJ mol$^{-1}$ on going from the neutral species to the cation[13,26]. Strong interactions between the rylene subunit and the glass substrate[27] or twisting of the rylene relative to the aryl subsitutent[24,28] associated with charge transfer are also possible contributing factors. Although **2** and **3** will be in the excited singlet state <1% of the time with the excitation rates here ($1 \times 10^6$ s$^{-1}$; Supplementary Section 7), dark charge transfer states[22] and the effects of local photoinduced reorganization of the viscous matrix[29] may persist much longer, accounting for the biased diffusion observed.

In summary, we have used defocused fluorescence imaging to observe the motions of single rylene derivatives **1**–**3** at a glass substrate, tuning their orientation and rotational dynamics with polymer overlayer viscosity. Derivatives **1**–**3** were designed to minimize overall flexibility and allow only well-defined conformational changes at specific bonds, so we could draw definitive conclusions regarding diffusion behaviour (unlike a previous study[30]). Most significantly, we could preferentially align rotors **2** and **3** using light. This is attributed not to rotation using optical torque, but to a photoinduced intramolecular charge transfer that inhibits diffusion, and thus biases the otherwise random rotation if excitation polarization is elliptical in the plane of rotation. It is precisely here where a macroscopic rotor analogy disconnects with our nanoscale equivalent. Fluctuating-friction rotors can convert optical energy to work, for instance by lowering the threshold for photoinduced orientation of liquid crystals[8], but rotation to the preferred plane can occur in either direction with equal probability. Further tailoring of the optical field distribution and medium conditions opens possibilities to rotate these molecular rotors directionally via orientational ratcheting.

Received 9 May 2013; accepted 25 November 2013; published online 19 January 2014

## References


1. Van Delden, R. A. *et al.* Unidirectional molecular motor on a gold surface. *Nature* **437,** 1337–1340 (2005).
2. Perera, U. G. E. *et al.* Controlled clockwise and anticlockwise rotational switching of a molecular motor. *Nature Nanotech.* **8,** 46–51 (2013).
3. Vogelsberg, C. S. & Garcia-Garibay, M. A. Crystalline molecular machines: function, phase order, dimensionality, and composition. *Chem. Soc. Rev.* **41,** 1892–1910 (2012).
4. Nguyen, T. *et al.* A reversible molecular valve. *Proc. Natl Acad. Sci. USA* **102,** 10029–10034 (2005).
5. Browne, W. R. & Feringa, B. L. Making molecular machines work. *Nature Nanotech.* **1,** 25–35 (2006).
6. Astumian, R. D. Thermodynamics and kinetics of a Brownian motor. *Science* **276,** 917–922 (1997).
7. Barrell, M. J., Campaña, A. G., von Delius, M., Geertsema, E. M. & Leigh, D. A. Light-driven transport of a molecular walker in either direction along a molecular track. *Angew. Chem. Int. Ed.* **50,** 285–290 (2011).
8. Jánossy, I. Optical reorientation in dye-doped liquid crystals. *J. Nonlin. Opt. Phys. Mater.* **8,** 361–377 (1999).
9. Kreuzer, M., Benkler, E., Paparo, D., Casillo, G. & Marrucci, L. Molecular orientation by photoinduced modulation of rotational mobility. *Phys. Rev. E* **68,** 011701 (2003).
10. Michl, J. & Sykes, E. C. H. Molecular rotors and motors: recent advances and future challenges. *ACS Nano* **3,** 1042–1048 (2009).
11. Coronado, E., Gaviña, P. & Tatay, S. Catenanes and threaded systems: from solution to surfaces. *Chem. Soc. Rev.* **38,** 1674–1689 (2009).
12. Balzani, V., Credi, A. & Venturi, M. Molecular machines working on surfaces and at interfaces. *ChemPhysChem* **9,** 202–220 (2008).
13. Toyota, S. Rotational isomerism involving acetylene carbon. *Chem. Rev.* **110,** 5398–5424 (2010).
14. Böhmer, M. & Enderlein, J. Orientation imaging of single molecules by wide-field epifluorescence microscopy. *J. Opt. Soc. Am. B* **20,** 554–559 (2003).
15. Deres, A. *et al.* The origin of heterogeneity of polymer dynamics near the glass temperature as probed by defocused imaging. *Macromolecules* **44,** 9703–9709 (2011).
16. Uji-i, H. *et al.* Visualizing spatial and temporal heterogeneity of single molecule rotational diffusion in a glassy polymer by defocused wide-field imaging. *Polymer* **47,** 2511–2518 (2006).
17. Lu, C-Y. & Vanden Bout, D. A. Effect of finite trajectory length on the correlation function analysis of single molecule data. *J. Chem. Phys.* **125,** 124701 (2006).
18. Mackowiak, S. A. & Kaufman, L. J. When the heterogeneous appears homogeneous: discrepant measures of heterogeneity in single-molecule observables. *J. Phys. Chem. Lett.* **2,** 438–442 (2011).
19. Wakelin, S. & Bagshaw, R. A prism combination for near isotropic fluorescence excitation by total internal reflection. *J. Microsc.* **209,** 143–148 (2003).
20. Osborne, M. A., Balasubramaniam, S., Furey, W. S. & Klenerman, D. Optically biased diffusion of single molecules studied by confocal fluorescence microscopy. *J. Phys. Chem. B* **102,** 3160–3167 (1998).
21. Manzo, C., Paparo, D. & Marrucci, L. Photoinduced random molecular reorientation by non-radiative energy relaxation: an experimental test. *Phys. Rev. E* **70,** 051702 (2004).
22. Flors, C. *et al.* Energy and electron transfer in ethynylene bridged perylene diimide multichromophores. *J. Phys. Chem. C* **111,** 4861–4870 (2007).
23. Li, C. *et al.* Rainbow perylene monoimides: easy control of optical properties. *Chem. Eur. J.* **15,** 878–884 (2009).
24. Andrew, T. L. & Swager, T. M. Thermally polymerized rylene nanoparticles. *Macromolecules* **44,** 2276–2281 (2011).
25. Margineanu, A. *et al.* Visualization of membrane rafts using a perylene monoimide derivative and fluorescence lifetime imaging. *Biophys. J.* **93,** 2877–2891 (2007).
26. Okuyama, O., Cockett, M. C. R. & Kimura, K. Observation of torsional motion in the ground-state cation of jet-cooled tolane by two-color threshold photoelectron spectroscopy. *J. Chem. Phys.* **97,** 1649–1654 (1992).
27. Daniels, C. R., Reznik, C. & Landes, C. F. Dye diffusion at surfaces: charge matters. *Langmuir* **26,** 4807–4812 (2010).

28. Kirmaier, C. *et al.* Excited-state photodynamics of perylene-porphyrin dyads. 5. Tuning light-harvesting characteristics via perylene substituents, connection motif, and three-dimensional architecture. *J. Phys. Chem. B* **114,** 14249–14264 (2010).
29. Karageorgiev, P. *et al.* From anisotropic photo-fluidity towards nanomanipulation in the optical near-field. *Nature Mater.* **4,** 699–703 (2005).
30. Nishimura, D. *et al.* Single-molecule imaging of rotaxanes immobilized on glass substrates: observation of rotary movement. *Angew. Chem. Int. Ed.* **120,** 6077–6079 (2008).

## Acknowledgements

The research leading to these results received funding from the European Research Council under the European Union's Seventh Framework Programme (FP7/2007-2013/ERC grant agreement 291593 FLUOROCODE), from the Flemish government in the form of a long-term structural funding 'Methusalem' grant (METH/08/04 CASAS), from the 'Fonds voor Wetenschapplijk Onderzoek Vlaanderen' (FWO grants G0413.10, G0697.11 and G0197.11), from the Hercules Foundation (HER/08/021) and from the Federal Science Policy of Belgium (IAP-PAI P7/05 'Functional Supramolecular Systems') and the UNIK research initiative of the Danish Ministry of Science, Technology and Innovation (grant 09-065274).

## Author contributions

K.M., A.H., J.H. and F.D.S. devised the project. S.M., H.N., C.L. and A.B. synthesized the molecules. J.A.H., A.D., S.R., H.U. and T.V. carried out optical measurements. J.E. and H.U. wrote the analysis software. J.A.H. analysed the data and wrote the paper. All authors discussed the results and commented on the manuscript.

## Additional information

Supplementary information is available in the online version of the paper. Reprints and permissions information is available online at www.nature.com/reprints. Correspondence and requests for materials should be addressed to H.U. and J.H.

## Competing financial interests

The authors declare no competing financial interests.